Journal of Visualized Experiments

Deep and spatially controlled volume ablations using a two-photon microscope in the zebrafish gastrula.

--Manuscript Draft--

Article Type:	Invited Methods Collection - JoVE Produced Video
Manuscript Number:	JoVE62815R1
Full Title:	Deep and spatially controlled volume ablations using a two-photon microscope in the zebrafish gastrula.
Corresponding Author:	Nicolas David Laboratory for Optics and Biosciences, CNRS UMR7645, INSERM U1182, Institut Polytechnique de Paris Palaiseau, Essonne FRANCE
Corresponding Author's Institution:	Laboratory for Optics and Biosciences, CNRS UMR7645, INSERM U1182, Institut Polytechnique de Paris
Corresponding Author E-Mail:	nicolas.david@polytechnique.edu
Order of Authors:	Arthur Boutillon
	Sophie Escot
	Nicolas David
Additional Information:	
Question	**Response**
Please specify the section of the submitted manuscript.	Developmental Biology
Please indicate whether this article will be Standard Access or Open Access.	Standard Access ($1400)
Please indicate the **city, state/province, and country** where this article will be **filmed**. Please do not use abbreviations.	Palaiseau, Essonne, France
Please confirm that you have read and agree to the terms and conditions of the author license agreement that applies below:	I agree to the Author License Agreement
Please provide any comments to the journal here.	

TITLE:

Deep and Spatially Controlled Volume Ablations Using a Two-Photon Microscope in the Zebrafish Gastrula

AUTHORS AND AFFILIATIONS:

Arthur Boutillon, Sophie Escot, Nicolas B. David

Laboratory for Optics and Biosciences, CNRS UMR7645, INSERM U1182, Institut Polytechnique de Paris, 91128 Palaiseau, France.

Corresponding Author:
Nicolas B. David (nicolas.david@polytechnique.edu)

Email addresses of co-authors:
Arthur Boutillon (arthur.boutillon@polytechnique.edu)
Sophie Escot (sophie.escot@polytechnique.edu)
Nicolas B. David (nicolas.david@polytechnique.edu)

SUMMARY:

Embryonic development requires large-scale coordination of cell motion. Two-photon excitation mediated laser ablation allows the spatially controlled 3-dimensional ablation of large groups of deep cells. In addition, this technique can probe the reaction of collectively migrating cells *in vivo* to perturbations in their mechanical environment.

ABSTRACT:

Morphogenesis involves many cell movements to organize cells into tissues and organs. For proper development, all these movements need to be tightly coordinated, and accumulating evidence suggests this is achieved, at least in part, through mechanical interactions. Testing this in the embryo requires direct physical perturbations. Laser ablations are an increasingly used option that allows relieving mechanical constraints or physically isolating two cell populations from each other. However, many ablations are performed with an ultraviolet (UV) laser, which offers limited axial resolution and tissue penetration. A method is described here to ablate deep, significant, and spatially well-defined volumes using a two-photon microscope. Ablations are demonstrated in a transgenic zebrafish line expressing the green fluorescent protein in the axial mesendoderm and used to sever the axial mesendoderm without affecting the overlying ectoderm or the underlying yolk cell. Cell behavior is monitored by live imaging before and after the ablation. The ablation protocol can be used at different developmental stages, on any cell type or tissue, at scales ranging from a few microns to more than a hundred microns.

INTRODUCTION:

Cell-cell interactions play vital roles in development. Cells provide signals that their direct neighbors or cells can perceive at a distance, thereby influencing their fate and/or behavior. Many of these signals are chemical in nature. For instance, in the well-characterized induction

events, one cell group produces diffusible molecules affecting the fate of another cell population[1]. Other signals, however, are mechanical; cells exert forces and constraints on their neighbors, which the neighbors perceive and respond to[2].

One way of studying the importance of these cell-cell interactions *in vivo* is to eliminate some cells and observe subsequent development. Unfortunately, available techniques to remove or destroy cells are limited. Cells can be removed surgically[3,4], using needles or small wires, but such treatments are invasive, not very precise, and usually performed under a stereomicroscope, preventing immediate imaging under a microscope. Furthermore, targeting deep cells implies piercing a hole in overlying tissues, creating unwanted perturbations. Genetically encoded photosensitizers, such as KillerRed, have been used to induce cell death via light illumination[5]. Photosensitizers are chromophores that generate reactive oxygen species upon light irradiation. Their main limitation is that they require long light illuminations (around 15 min), which may be difficult to achieve if cells are moving, and that they induce cell death through apoptosis, which is not immediate.

Finally, laser ablations have been developed and widely used in the past 15 years[6–12]. A laser beam is focused on the targeted cell/tissue. It induces its ablation through heating, photoablation, or plasma-induced ablation; the involved process depends on the power density and exposure time[13]. Most ablation protocols use UV lasers for their high energy. However, UV light is both absorbed and scattered by biological tissues. Thus, targeting deep cells requires a high laser power, which then induces damages in more superficial, out-of-plane tissues. This limits the use of UV lasers to superficial structures and their relatively low axial resolution. Non-linear optics (so-called two-photon microscopy) uses non-linear properties of light to excite a fluorophore with two photons of approximately half-energy in the infrared domain. When applied to ablations, this has three main advantages. First, the infrared light is less scattered and less absorbed than UV light by biological tissues[14], allowing to reach deeper structures without increasing the required laser power. Second, the use of a femtosecond pulsed laser provides very high power densities, creating an ablation through plasma induction, which, contrary to heating, does not diffuse spatially[15]. Third, the power density inducing plasma formation is reached at the focal point only. Thanks to these properties, two-photon laser ablations can be used to precisely target deep cells without affecting the surrounding tissue environment.

Collective migrations are an excellent example of developmental processes in which cell-cell interactions are fundamental. Collective migrations are defined as cell migrations in which neighboring cells[16] influence the behavior of one cell. The nature of these interactions (chemical or mechanical) and how they affect cell migration can vary greatly and is often not entirely understood. The ability to remove cells and observe how this affects the others is critical in further unraveling these collective processes. A few years ago, we established—using surgical approaches—that the migration of the polster during zebrafish gastrulation is a collective migration[17]. The polster is a group of cells that constitutes the first internalizing cells on the dorsal side of the embryo[18]. These cells, labeled in green in the *Tg(gsc:GFP)* transgenic line, are located deep in the embryo, below several layers of epiblast cells. During gastrulation, this group leads the extension of the axial mesoderm, migrating from the embryonic organizer to the animal

pole[19–23] (**Figure 1A**). We established that cells require contact with their neighbors to orient their migration in the direction of the animal pole. However, better understanding the cellular and molecular bases of this collective migration involves removing some cells to see how this influences the remaining ones. We, therefore, developed ablations of large and deep volumes using a two-photon microscopy setup. Here, we demonstrate the use of this protocol to sever the polster in its middle and observe the consequences on cell migration by tracking nuclei labeled with Histone2B-mCherry and studying its expression.

PROTOCOL:

All animal work was approved by the Ethical Committee N 59 and the Ministère de l'Education Nationale, de l'Enseignement Supérieur et de la Recherche under the file number APAFIS#15859-2018051710341011v3. Some of the steps described below are specific to our equipment and software but could be easily adapted to different equipment.

1. Injection preparation

1.1. Prepare 75 mL of 1% agarose solution in the Embryo Medium (EM).

1.2. Place the injecting mold in a 90 mm Petri dish and pour approximately 50 mL of agarose, enough for the mold to float. Let the agarose solidify and remove the injecting mold.

1.3. Prepare an agarose-coated dish by pouring 1 mL of agarose in a 30 mm Petri dish.

1.4. Prepare 4 µL of 30 ng/µL Histone2B-mCherry mRNA solution by diluting the stock solution in RNase-free water and keep on ice.

NOTE: Take care to wear gloves while manipulating mRNA to avoid RNase-mediated degradation.

1.5. Pull an injection needle from a capillary using the micropipette puller.

2. Embryo preparation

2.1. Once fishes have laid eggs, collect, rinse, and harvest in a 90 mm Petri dish in EM. Place the embryos in a 28.5 °C incubator.

2.2. Wait 20 min for the first cell to become visible.

2.3. Transfer 30 embryos to the injection plate filled with EM. Squeeze embryos in the grooves using slightly blunt forceps and orient them with the animal pole up.

2.4. Using a microloader tip, fill an injection needle with 2 µL of mRNA solution. Insert the needle in the capillary holder placed in a micro-manipulator connected with polytetrafluoroethylene (PTFE) tubing to an air injector.

2.5. Under the stereomicroscope, carefully break the tip of the needle.

2.6. Inject the mRNA solution in the 1-cell stage embryos by inserting the needle in the cell.

NOTE: The volume injected is approximately one-third of the cell volume.

2.7. Place back injected embryos in the 28.5 °C incubator.

3. Preparation of the two-photon microscope

NOTE: Two lasers are used in this protocol. One is used to image GFP (at 920 nm) and perform ablations (at 820 nm). It will be referred to as the green/ablation laser. The other is used at 1160 nm to image mCherry. It will be referred to as the red laser.

3.1. Set the green/ablation laser to 820 nm (ablation wavelength) and the red laser to 1160 nm (mCherry excitation).

3.2. Using movable mirrors on the optical path, align green/ablation and red laser beams both at the entry and exit of the scan head.

NOTE: This increases the laser beam focus and minimizes focal volume for excitation and ablation.

3.3. Measure the maximum power of the green/ablation laser at 820 nm under the objective. To do so, place the power meter under the objective, close the black chamber, set green/ablation laser power to 100%, and open the shutters. Compute the percentage of laser power needed to reach 300 mW.

3.4. Set back the green/ablation laser to 920 nm (GFP excitation) and set the laser power to 7%. Set the red laser power to 15%.

3.5. Activate epi-PhotoMultiplier Tubes (PMT) detectors for green and red lines; set green and red line PMT sensitivity to 65%.

3.6. Set the field of view to 400 x 400 µm, image resolution to 512 x 512 pixels, and scanning frequency to 800 Hz.

3.7. Select **3D Timelapse Imaging** mode. Then, create a folder and activate **Autosave** for data after each acquisition.

3.8. Assemble the heating chamber and set it to 28 °C. Wait at least 10 min for the chamber and the objective to warm.

4. Mounting the embryo

4.1. Under a fluorescence stereomicroscope, identify embryos at 70% epiboly that express GFP.

NOTE: Select embryos with a bright signal in the axial mesoderm and no background fluorescence for better imaging quality.

4.2. Transfer three to four selected embryos in the agarose coated dish (step 1.3) using a plastic Pasteur pipette and carefully dechorionate them using fine forceps.

NOTE: Dechorionated embryos are very delicate and will burst upon contact with air or plastic.

4.3. Pour 1 mL of 0.2% agarose in 1x penicillin-streptomycin EM in a small glass vial. Place the vial in a preheated 42 °C dry block heater.

NOTE: The following steps must be performed quickly to allow embryo orientation before agarose sets.

4.4. Transfer a dechorionated embryo in the 0.2% agarose glass vial using a fire-polished glass pipette. Take care not to add too much EM in the agarose to avoid diluting it. Discard the remaining EM from the pipette and aspirate the embryo back along with enough agarose to cover the slide of the glass bottom dish before the embryo falls out of the pipette.

4.5. Blow the agarose and the embryo on the glass slide of the dish. Take care not to let the embryo touch the air or the plastic side of the dish. Next, fill the chamber around the glass slide with agarose.

4.6. Use an eyelash to orient the embryo so that the targeted region is at the top (**Figure 1B**).

NOTE: When orienting embryos, take care to only touch the blastoderm, not the very fragile yolk. Agarose will set in around 1 min, depending on room temperature.

4.7. Wait ~5 min for the agarose to set completely, and then add a few drops of penicillin-streptomycin EM.

5. Locating the embryo and pre-ablation imaging

5.1. Place the glass bottom dish under the objective in the heated chamber. Immerse the objective in penicillin-streptomycin EM and close the heated chamber.

5.2. Move the slider to set the light path to oculars. Then, using oculars, fluorescent lamps, and stage control, find an embryo and set the focus to the surface of the embryo.

5.3. Turn the fluorescence lamp off, set the light path to PMTs, and close the black chamber.

NOTE: Be careful to turn off all light sources in the black chamber as it might damage the PMTs.

5.4. Start live imaging and locate axial mesoderm. Adjust the green/ablation and red laser powers to have a good signal (i.e., between 1,000 and 20,000 photons per pixel for GFP expressing areas). Use the red channel to move the stage to the very top of the embryo and set this position as Z = 0.

5.5. Choose a time-step of 1 min and a Z-step of 2 µm. A Z-course of 110 µm is sufficient to encompass the whole polster and is acquired in less than 1 min with these settings. Set the first slice 15 µm above the axial mesoderm (in the more superficial ectoderm).

NOTE: The polster moves along a curved line so that the bottom slice of the Z-stack should be set 30 µm deeper than the polster deepest position to accommodate its movement during the time-lapse imaging (**Figure 1E**).

5.6. Record 10-15 min of pre-ablation movie.

[**Place Figure 1 here**]

6. Target location and laser ablation

6.1. Locate the polster contour on live imaging and, using the Electro-Optic Modulator Region of Interest (EOM ROI) tool, draw a 20 pixel (15 µm) large rectangle that spans the width of the polster. Place this rectangle in the middle of the polster (**Figure 1E**).

6.2. Note the axial position of the highest and lowest planes containing polster cells. Ablations will be performed every 10 µm in between these two planes. Take care that the ROI does not overlap the yolk cell on any of these planes.

6.3. Place the stage at the lowest Z position of the interval. Ablations must be performed bottom-up as debris absorb light.

6.4. Set the green/ablation laser wavelength to 820 nm and set the **Power Percentage** to obtain an exit power of 300 mW (step 3.3).

6.5. Set the **Imaging Frequency** to 200 Hz.

6.6. Set green/ablation laser imaging EOM to 0 and select **ROI-Treat** mode.

6.7. Turn on the EOM and set the treatment to start immediately (after 0 frame).

6.8. Set the **Imaging Mode** to Timelapse and de-activate **Autosave**.

6.9. Set the **Time Step** to Fast mode.

6.10. Set the **Number of Treatment Frames** and **Number of Frames** to the value corresponding to the targeted depth (**Table 1**).

[**Place Table 1 here**]

6.11. Start imaging. The acquisition is black as the shutter to PMT closes during EOM treatment.

6.12. Move up the stage to the next Z position of the list (step 6.2).

6.13. Repeat steps 6.10 to 6.12 until the top of the polster is reached.

7. Post-ablation verification and imaging

7.1. Set the green/ablation laser to 920 nm and 5% power. Set the green/ablation laser imaging EOM to 100 and select the **Fullfield** mode.

7.2. Set the **Imaging Frequency** to 800 Hz. Turn EOM off.

7.3. Go through the whole stack in live mode to check whether every plane has been ablated. If this is not the case, go back to step 7.2.

NOTE: Ablation sometimes induces a vertical shift of neighboring tissues so that the Z-stack might have to be redefined.

7.4. Set the **Imaging Mode** to 3D Timelapse and re-activate **Autosave**. Record 40–60 min of post-ablation movie.

7.5. Check, in the post-ablation movie, whether the targeted cells were effectively ablated. Fluorescence recovery, or targeted cells occupying space and preventing follower cells from moving through, indicate that targeted cells were only photobleached and not ablated (**Figure 1E and Figure 2A**).

[**Place Figure 2 here**]

8. Data analysis

8.1. Open time-lapse series with the image analysis software and set correct pixel size.

8.2. In the **Spot** function, set the **Object Size** to 10 µm, as this is the average nucleus size during gastrulation. Then, run the **Spot** function to detect and track the nuclei.

NOTE: Detection may be slightly improved by considering the lower axial resolution, fitting a 12

µm long ellipsoidal shape along the Z-axis.

8.3. Use filters to remove false positives. In the *Tg(Gsc:GFP)* line, cells from the embryonic axis and some endodermal cells are labeled in green. Hence, filtering on green intensity allows a quick selection of these cells (**Figure 3A**).

8.4. Set the maximal distance between consecutive points to a value compatible with the speed of the cells.

NOTE: Be careful to consider the time interval between two frames. Polster cells migrate at 2.8 ± 0.8 µm/min. Hence, allowing 4 µm of maximum displacement for a time step of 1 min removes most artefactual tracks.

8.5. Allowing gaps over one or two time points provides longer continuous tracks but may introduce tracking errors. If a nucleus is not detected correctly at a one-time point, consider re-running spot detection with different parameters/filters.

8.6. Visually check tracks and, if necessary, correct them.

8.7. Export the results as a .xlsx file. Process the file using published spreadsheet routines[24] (**Figure 3B**) and custom routines on data analysis software (available on request).

[**Place Figure 3 here**]

REPRESENTATIVE RESULTS:

To sever the polster in its middle, a *Tg(gsc:GFP)* embryo, injected with Histone2B-mCherry mRNAs was mounted at the 70% epiboly stage, as described in step 4. The polster was identified by GFP expression, and the embryo was mounted so that the plane of the polster is perpendicular to the optical axis (**Figure 1B**). Tilting the embryo away from this position will complicate the procedure. The light will have to go through more tissues to reach the planes ablated, and ablation planes will be tilted relative to embryonic axes. Having verified that all the cell nuclei are correctly labeled, a 10 min pre-ablation time-lapse was recorded to capture cell movements before ablation (**Figure 1E and Figure 3A**, **Movie S1**).

The polster was morphologically identified, and a rectangular area of 15 µm x 200 µm, located in its middle, was ablated on five focal planes to ensure severing on the whole depth of the polster (**Figure 1E**, **Movie S1**). Imaging was restarted right after ablation and used to monitor the efficiency of the procedure. If successful, the ablation will have eliminated all cellular structures and GFP and mCherry fluorescence so that the ablated volume should appear as a signal-free volume. However, some debris may be created. This debris is autofluorescent, both in the green and red channels, and usually displays irregular elongated shapes parallel to the direction of ablation (**Figure 1E**). A too intense treatment will lead to forming any debris that may act as obstacles and perturb cell behavior. Even more potent treatments will induce cavitation, marked by the formation of bubbles in the tissue (**Figure 2B**). Cavitation is associated with a mechanical

shock wave propagating in tissues and may induce damages out of the targeted volume[13,15]. Embryos with cavitation bubbles should be discarded, and treatment should be tuned down by performing fewer treatment frames.

Conversely, too little treatment may photobleach fluorophores without inducing plasma formation, hence without ablating (**Figure 2A**). Incomplete photobleaching can easily be spotted by the presence of dim fluorescence with a characteristic cellular shape (**Figure 2A**). Such embryos should be discarded or treated again with a more potent treatment. Complete photobleaching is more challenging to differentiate from successful ablation, as both would result in a signal-free volume. Photobleaching can, however, be identified retrospectively, as fluorescence will progressively recover in the course of the post-ablation imaging. This, however, implies that non-ablated embryos are imaged for at least half an hour, which is time-consuming. We, therefore, suggest adjusting the treatment intensity (by increasing the number of treatments) to induce the formation of few visible debris, which will not affect cell behavior but immediately confirm effective ablation. Finally, the absence of damage in cells surrounding the ablation volume should be checked on the first post-ablation images (**Figure 2A**). Suppose laser treatment is tuned correctly (formation of few debris). In that case, damages in neighboring tissues are unlikely to result from the spatial spreading of the ablation, which is very well spatially defined, but rather result from inaccurate selection of the region to be ablated and/or tissue movements in the time between target selection and ablation. Embryos with affected neighboring tissues should be discarded.

After successful ablation, Z-stacks were captured every minute for 40 min, recording both the GFP cytoplasmic signal and the mCherry nuclear signal. Nuclei were then tracked, and their movement was used as a proxy for cell movement. Tracks corresponding to polster cells were identified on strong GFP signals (**Figure 3A**, Movie S1). The persistence of cell movement was measured by computing the cell direction auto-correlation[24]. Focusing on polster cells located in the anterior half of the polster revealed that severing the polster in its middle, thus separating these cells from the posterior part of the polster, decreased their direction autocorrelation (**Figure 3B**), demonstrating that proper migration of polster cells requires integrity of the whole polster, in line with its demonstrated collective migration[17].

After acquiring the post-ablation movie, embryos can be unmounted, carefully extracting them from the agarose using fine forceps, and incubated at 28.5 °C until they reach 24 h post-fertilization. Again, embryos should survive and should not present any apparent morphological defect (**Figure 1C,D**).

FIGURE AND TABLE LEGENDS:

Figure 1: **Successful outcome of laser ablations.** (**A**) Scheme of a gastrulating embryo at 70% epiboly in dorsal view; pAM: posterior axial mesoderm; black arrow marks the direction of polster migration; black square indicates a typical field of view for ablations in the polster. (**B**) Scheme of embryo mounting for polster severing. Lateral view. The embryo is mounted such that the plane of the polster is perpendicular to the optical axis: survival (**C**) and morphology (**D**) of control and

ablated embryos at 24 h post-fertilization. Scale bar is 300 µm. (**E**) Time sequence from laser ablation in the polster of a *Tg(gsc:GFP)* embryo expressing Histone2B-mCherry. Views with the green channel only are maximum projections. The close-up displays the ablated area containing cell debris. Views with green and red (displayed as magenta) channels are XY and XZ slices before and after ablation (the green lightning bolt represents ablation). XZ slices show that the overlying tissues (magenta nuclei without GFP expression) have not been affected by the ablation of underlying structures. The yellow dashed box corresponds to the ROI selected for laser ablation treatment. The scale bar is 50 µm in large views and 25 µm in the close-up.

Figure 2: **Negative results of laser ablations.** (**A**) Typical examples of potential failures in laser ablation. Large XY views are maximum projections, XZ view is a reconstructed section. Laser treated area comprises the two white arrowheads. Three focal planes are highlighted in the reconstructed section and displayed on the right. They correspond to three different kinds of failures. Plane 1 shows that cells above the polster have been ablated. This can be identified by the presence of autofluorescent debris on this focal plane (see close-up) above the polster (see position of plane 1 on the reconstructed section). This likely results from an incorrect definition of the region to be ablated. Plane 2 shows cells that have been bleached but not ablated. They can be identified as the low fluorescence signal still reveals intact cell contours (see close-up). Plane 3 displays intact cells, which have hardly been bleached by laser treatment. This could result from an incorrect definition of the region to be ablated or from poor treatment. In the situations depicted in planes 2 and 3, it is possible to re-apply a therapy to ablate the targeted cells. The scale bar is 50 µm in large views and 20 µm in close-ups. (**B**) A typical example of bubbles (marked by white asterisks) formed by cavitation is intense laser treatment. Such bubbles are not limited to a Z-plane, sometimes even spanning the full height of the polster, deforming neighboring tissues. The scale bar is 50 µm.

Figure 3: **Isolation of the anterior half of the polster affects cell directionality.** (**A**) 3D reconstructions a *Tg(gsc:GFP)* embryo expressing Histone2B-mCherry (displayed in magenta), before and after a laser ablation severing the polster in its middle. Nuclei belonging to the anterior half of the polster are marked with a magenta dot and tracked over time before and after ablation (see **Movie S1**). The scale bar is 50 µm. (**B**) As a measure of migration persistence, direction auto-correlation of cells belonging to the anterior part of the polster before and after ablation. Cells display a continuous motion before ablation, which drastically decreases after ablation, indicating loss of collective-oriented migration. Direction auto-correlation was also measured on cells forming the anterior half of the polster of a non-ablated embryo, as a control. The graph envelopes indicate standard error.

Table 1: Suggested number of laser treatment frames as a function of targeted cell depth in the embryo (0 being the embryo's surface).

Movie S1: **Successful laser ablation.** Laser ablation in the middle of the polster of a *Tg(gsc:GFP)* embryo expressing Histone2B-mCherry. Nuclei from the anterior part of the polster are tracked over time and marked by magenta dots. Tracks are time color-coded (**Figure 3**). Empty frames correspond to laser ablation.

DISCUSSION:

Here, we describe a protocol that uses non-linear optics to perform deep and spatially well-defined volume ablations. The most critical step of the protocol is to find treatment conditions that provide sufficient energy to allow ablations, but not too much energy, to avoid excessive debris or cavitation. The amount of delivered energy at the target site mainly depends on: (1) the laser exit power, (2) the quality of laser alignment, (3) the nature of the tissue to be ablated, (4) the depth of targeted tissues. Therefore, before each experiment, it is crucial to measure laser exit power, adjust it to a reference value (300 mW at 820 nm in our protocol), and ensure proper laser alignment. Under these assumptions, treatment conditions should be reproducible from one experimental day to another. We recommend performing extensive tests to define optimal parameters (laser power and number of treatment frames) for a specific sample type. These parameters can then be used in all similar experiments. In the example described here (severing of the polster during gastrulation), we have, for instance, established treatment conditions for ablations at different depths within the embryo (**Table 1**) and now rely on this chart when performing experiments. Of note, the 820 nm wavelength was chosen as it is, on our system, the wavelength providing the highest peak energies (due to laser and optics properties). Shorter or longer wavelengths could be used depending on system properties[6,11,12]. Depth of the targeted tissue being a critical parameter, embryo mounting is also a crucial step, as incorrect mounting may increase tissue thickness that light must pass through to reach the target volume.

One of the original features of the described protocol is to ablate an entire volume by performing successive ablations on different focal planes. Since ablations will generate debris that absorbs light, we identified that it is crucial to start ablation on the most profound plane and sequentially ablate from the deepest to the most superficial plane.

This protocol describes the ablation of deep and large volumes and the recording of neighboring tissue response within minutes after ablation to over an hour. One of the potential limitations of the protocol is the time required to perform ablation and restart imaging. Two factors limit this delay. The first one is the time needed to perform ablations on multiple focal planes. On our system, severing of the polster is performed by a trained user in 2–3 min. This could be reduced by optimizing the software to automate the ablation on different planes. Still, total ablation time will equal the time required to scan the target region, times the number of repetitions on each focal plane, times the number of focal planes, which, in our conditions, is about 1 min. Considering cell migration speed, this means that some cells may enter or exit the targeted area during the ablation procedure. In our case, this did not prove to be an issue but could be if an absolute precision in cell targeting is required. The second limiting factor is that the same laser is used to perform ablation (at 820 nm) and excite green fluorophore (at 920 nm). The delay between the last ablation and the start of recording is thus defined by the time required to tune the laser from 820 nm to 920 nm, ranging from 30 s to 1 min.

In some cases, in particular, for smaller ablations (single-cell ablation, ablations of subcellular components such as cytoskeleton elements), recording the immediate response of the cell/tissue may be critical to infer its mechanical state[25–27]. In such cases, the limitation could be

circumvented, either by imaging with another laser (here, for instance, recording only red signals with the 1160 nm laser, using a third laser line) or imaging green fluorophore at 820 nm. This is not the optimal wavelength for imaging (limited excitation of fluorophores, strong photo-toxic effects) but could be used over short periods to record immediate tissue response.

Few techniques are available to eliminate cells and see how this affects the rest of the embryo. The two main options are to remove cells physically or to destroy them, as in laser ablations. Compared to physical removal, cell destruction may release cytoplasmic content, which can influence neighboring cells. This was historically highlighted by the controversy and diverging results obtained by Wilhelm Roux and Hans Driesch regarding the mosaic or regulative development of the frog and sea urchin embryo[28]. More recently, differences have been observed in wound healing assays, depending on whether the wound is created by scratch (which destroys some cells) or removing an insert[29]. However, physically removing cells without damaging other tissues is only possible for cells at the very surface of the embryo and cells that are not too adherent to their neighbors, thus limiting the range of such approaches. Consequently, different strategies have been developed to destroy cells, laser ablations being the most employed. UV laser ablations have been and are increasingly used, in particular, to perform small, superficial ablations, and observe immediate tissue response.

We here described the use of infrared light to perform deeper and spatially well-defined ablations. The main limitation of this protocol is the requirement for an infrared pulsed laser and a two-photon imaging setup. However, such equipment is becoming more and more frequent on imaging platforms. In addition, the EOM used here to ablate one region in the image selectively could be replaced by fluorescence recovery after the photobleaching (FRAP) module. Though less convenient, it could even be possible to perform the protocol without EOM nor FRAP modules by simply zooming on the targeted area[10]. Such a pulsed infrared laser brings two main advantages compared to most classical ablation protocols. First, thanks to the efficient penetration of infrared light in living tissues, deep focal planes can be reached with laser powers that do not induce out-of-focus damages. This allowed us to target cells as deep as 120 µm, out of reach with one-photon excitation protocols. Second, the use of non-linear optics ensures excellent axial resolution, permitting precisely controlled 3D ablations, even at depth in the tissue. Combining these two advantages allows ablation of specifically defined, deep, and eventually large volumes.

We describe using a two-photon microscope to sever the polster, an experiment we and others recently performed[30]. With few adjustments, the proposed protocol could, however, be adapted to many different samples. We have, for instance, successfully used it to perform complete ablation of the polster, ablations within the lateral mesoderm during gastrulation, or ablations of individual Schwan cells during their migration on their associated axon, without affecting the axon. We, therefore, believe this protocol is a valuable and versatile tool, which should be helpful in many experimental systems to analyze the impact of some cells/tissues on the behavior and development of the neighboring structures.

ACKNOWLEDGMENTS:

We thank Emilie Menant for fish care, the Polytechnique Bioimaging Facility for assistance with live imaging on their equipment partly supported by Région Ile-de-France (interDIM) and Agence Nationale de la Recherche (ANR-11-EQPX-0029 Morphoscope2, ANR-10-INBS-04 France BioImaging). This work was supported by the ANR grants 15-CE13-0016-1, 18-CE13-0024, 20-CE13-0016, and the European Union's Horizon 2020 research and innovation programme under the Marie Skłodowska-Curie grant agreement No 840201, the Ministère de l'Enseignement Supérieur et de la Recherche and the Centre National de la Recherche Scientifique.

DISCLOSURES:

The authors declare no competing interests.

REFERENCES:

1. Slack, J. M. W. Embryonic induction. *Mechanisms of Development*. **41** (2–3), 91–107 (1993).
2. Fernandez-Sanchez, M.-E., Brunet, T., Röper, J.-C., Farge, E. Mechanotransduction's impact on animal development, evolution, and tumorigenesis. *Annual Review of Cell and Developmental Biology*. **31**, 373–397 (2015).
3. Shih, J., Fraser, S. E. Characterizing the zebrafish organizer: microsurgical analysis at the early-shield stage. *Development*. **122** (4), 1313–1322 (1996).
4. Selleck, M. A. J. Culture and microsurgical manipulation of the early avian embryo. *Methods in Cell Biology*. **51** (51), 1–21 (1996).
5. Bulina, M.E. et al. A genetically encoded photosensitizer. *Nature Biotechnology*. **24** (1), 95–99 (2006).
6. Fang-Yen, C., Gabel, C. V., Samuel, A. D. T., Bargmann, C. I., Avery, L. Laser microsurgery in Caenorhabditis elegans. *Methods in Cell Biology*. **107**, 177–206 (2012).
7. Colombelli, J., Grill, S. W., Stelzer, E. H. K. Ultraviolet diffraction limited nanosurgery of live biological tissues. *Review of Scientific Instruments*. **75** (2), 472–478 (2004).
8. Smutny, M., Behrndt, M., Campinho, P., Ruprecht, V., Heisenberg, C.-P. UV laser ablation to measure cell and tissue-generated forces in the zebrafish embryo in vivo and ex vivo. *Methods in Molecular Biology (Clifton, N.J.)*. **1189**, 219–235 (2015).
9. Behrndt, M. et al. Forces driving epithelial spreading in zebrafish gastrulation. *Science*. **338** (6104), 257–260 (2012).
10. Volpe, B. A., Fotino, T. H., Steiner, A. B. Confocal microscope-based laser ablation and regeneration assay in zebrafish interneuromast cells. *Journal of Visualized Experiments: JoVE*. **2020** (159), 1–9 (2020).
11. Bonnet, I. et al. Mechanical state, material properties and continuous description of an epithelial tissue. *Journal of the Royal Society, Interface*. **9** (75), 2614–2623 (2012).
12. Rauzi, M., Lenne, P. F., Lecuit, T. Planar polarized actomyosin contractile flows control epithelial junction remodelling. *Nature*. **468** (7327), 1110–1115 (2010).
13. Niemz, M. H. *Laser-Tissue Interactions*. *Encyclopedia of Biomaterials and Biomedical Engineering, Second Edition - Four Volume Set*. Springer International Publishing. Cham (2019).
14. Smith, A. M., Mancini, M. C., Nie, S. Bioimaging: second window for in vivo imaging. *Nature Nanotechnology*. **4** (11), 710–711 (2009).
15. Rauzi, M., Lenne, P.-F. Cortical forces in cell shape changes and tissue morphogenesis.

Current Topics in Developmental Biology. **95**, 93–144 (2011).
16. Theveneau, E., David, N. B. Migrations cellulaires collectives. *Medecine/Sciences*. **30** (8–9), 751–757 (2014).
17. Dumortier, J. G., Martin, S., Meyer, D., Rosa, F. M., David, N. B. Collective mesendoderm migration relies on an intrinsic directionality signal transmitted through cell contacts. *Proceedings of the National Academy of Sciences of the United States of America*. **109** (42), 16945–16950 (2012).
18. Solnica-Krezel, L., Stemple, D. L., Driever, W. Transparent things: cell fates and cell movements during early embryogenesis of zebrafish. *BioEssays*. **17** (11), 931–939 (1995).
19. Montero, J.-A., Kilian, B., Chan, J., Bayliss, P. E., Heisenberg, C.-P. Phosphoinositide 3-kinase is required for process outgrowth and cell polarization of gastrulating mesendodermal cells. *Current Biology*. **13** (15), 1279–1289 (2003).
20. Ulrich, F. et al. Slb/Wnt11 controls hypoblast cell migration and morphogenesis at the onset of zebrafish gastrulation. *Development*. **130** (22), 5375–5384 (2003).
21. Kai, M., Heisenberg, C.-P., Tada, M. Sphingosine-1-phosphate receptors regulate individual cell behaviours underlying the directed migration of prechordal plate progenitor cells during zebrafish gastrulation. *Development*. **135** (18), 3043–3051 (2008).
22. Smutny, M. et al. Friction forces position the neural anlage. *Nature Cell Biology*. **19** (4), 306–317 (2017).
23. Johansson, M., Giger, F. A., Fielding, T., Houart, C. Dkk1 controls cell-cell interaction through regulation of non-nuclear β-Catenin pools. *Developmental Cell*. **51** (6), 775–786.e3 (2019).
24. Gorelik, R., Gautreau, A. Quantitative and unbiased analysis of directional persistence in cell migration. *Nature Protocols*. **9** (8), 1931–1943 (2014).
25. Grill, S. W., Howard, J., Schäffer, E., Stelzer, E. H. K., Hyman, A. A. The distribution of active force generators controls mitotic spindle position. *Science (New York, N.Y.)*. **301** (5632), 518–521 (2003).
26. Desprat, N., Supatto, W., Pouille, P.-A. A., Beaurepaire, E., Farge, E. Tissue deformation modulates twist expression to determine anterior midgut differentiation in Drosophila embryos. *Developmental Cell*. **15** (3), 470–477 (2008).
27. Farhadifar, R., Röper, J.-C., Aigouy, B., Eaton, S., Jülicher, F. The influence of cell mechanics, cell-cell interactions, and proliferation on epithelial packing. *Current Biology*. **17** (24), 2095–2104 (2007).
28. Willier, B. H., Oppenheimer, J. M. *Foundations of Experimental Embryology*. Englewood Cliffs: Prentice-Hall (1964).
29. Ashby, W. J., Zijlstra, A. Established and novel methods of interrogating two-dimensional cell migration. *Integrative Biology: Quantitative Biosciences from Nano to Macro*. **4** (11), 1338–1350 (2012).
30. Bosze, B. et al. Pcdh18a regulates endocytosis of E-cadherin during axial mesoderm development in zebrafish. *Histochemistry and Cell Biology*. 154 (5), 463–480 (2020).

Figure 1

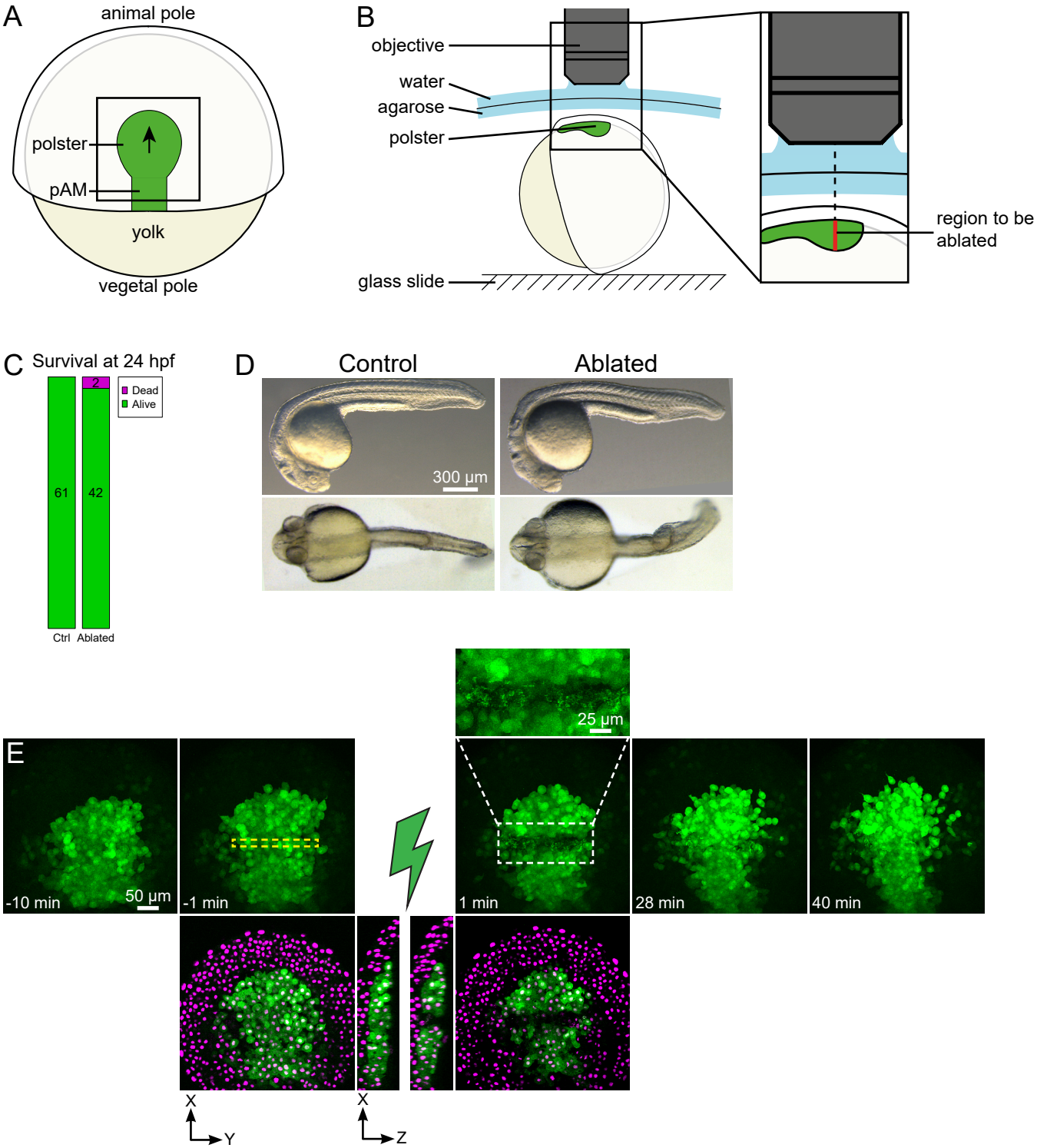

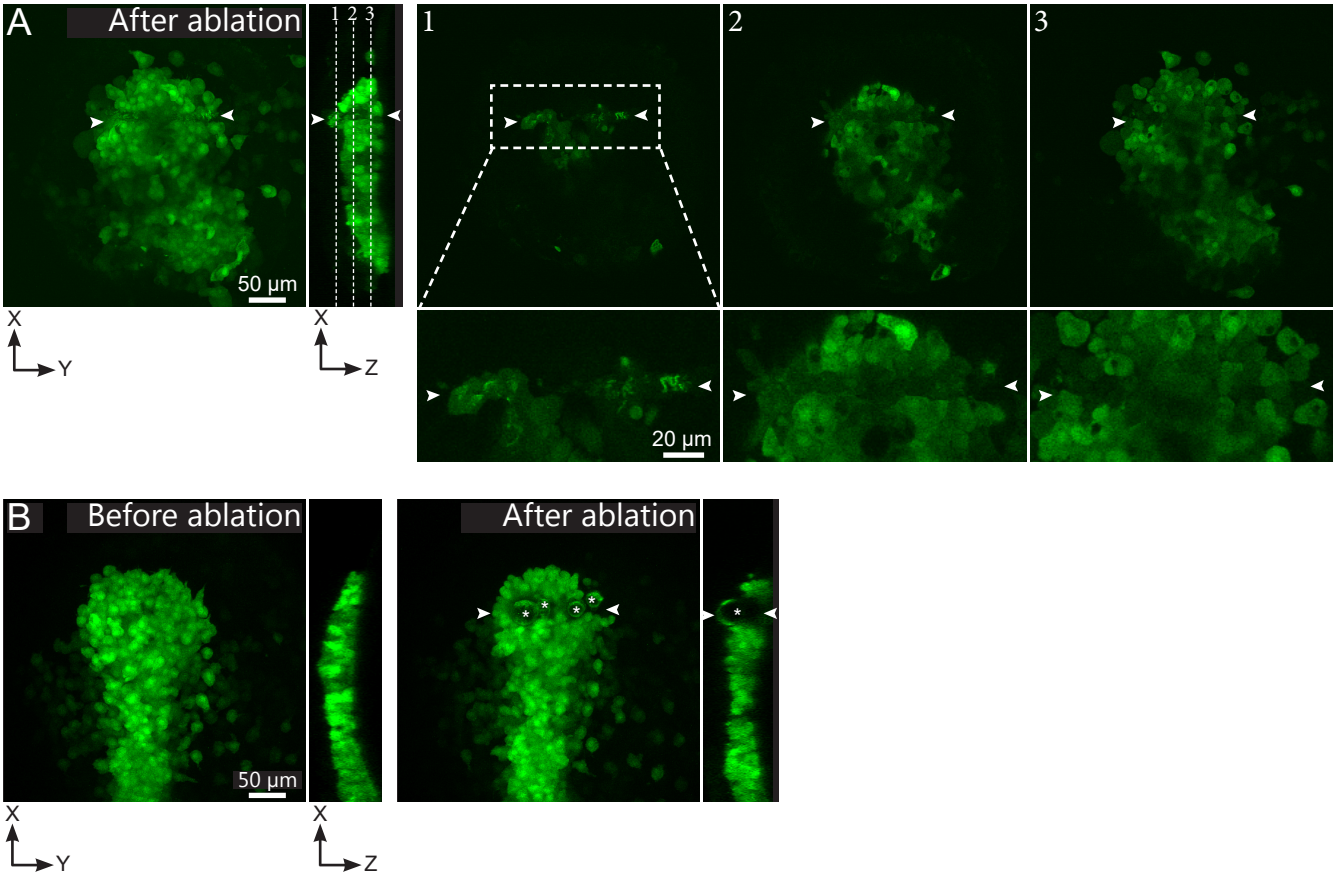

Figure 3

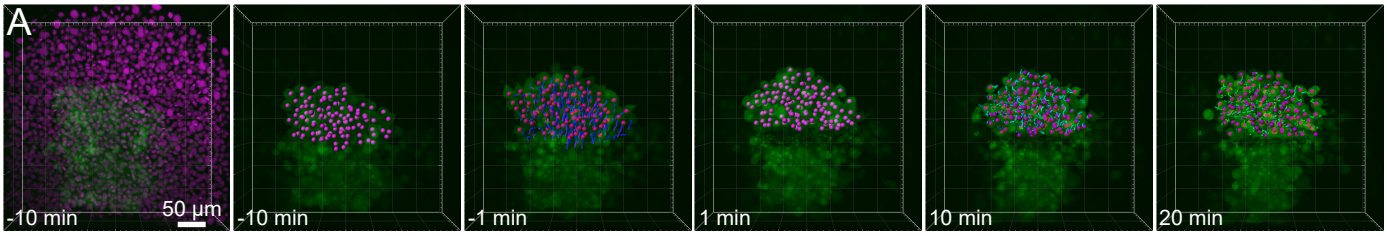

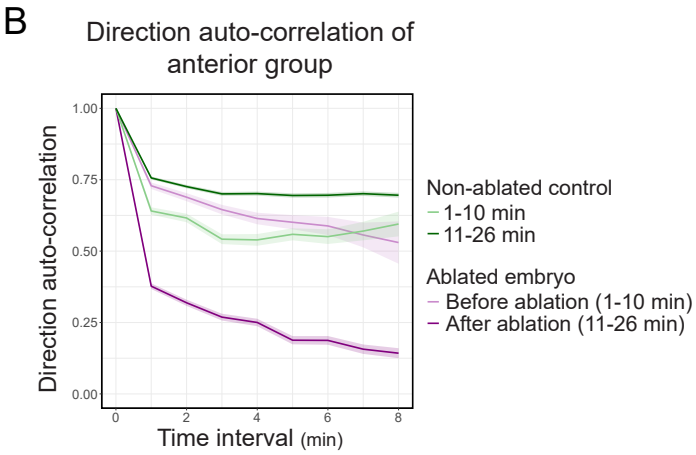

Movie S1

Click here to access/download

Video or Animated Figure

MovieS1.mp4

Table 1

Depth (µm)	Treatment frames
-30	1
-35	1-2
-40	1-2
-45	2
-50	2-3
-55	3
-60	3-4
-65	4
-70	4
-75	4-5
-80	4-5
-85	5
-90	5
-95	5-6
-100	6
-105	6

We are greatly thankful to the editor and the reviewers for their constructive suggestions. We have carefully considered each of them and have performed the requested modifications of the manuscript. We feel that this has improved the manuscript.

Editorial comments:

Changes to be made by the Author(s):

1. Please take this opportunity to thoroughly proofread the manuscript to ensure that there are no spelling or grammar issues. Please define all abbreviations at first use.

We did our best to spot potential spelling or grammar issues. All abbreviations are defined at first use.

2. Please provide an email address for each author.

Each author's email address was added in their affiliation.

3. Please revise the following lines to avoid overlap with previously published work: 82-83, 146-149 (convert 146-147 to a note and rephrase to avoid overlap; rephrase148-149 to avoid overlap), 226-227, 236-239.

These sentences were rephrased.

4. JoVE cannot publish manuscripts containing commercial language. This includes trademark symbols (™), registered symbols (®), and company names before an instrument or reagent. Please remove all commercial language from your manuscript and use generic terms instead. All commercial products should be sufficiently referenced in the Table of Materials and Reagents.
For example: IMARIS; Microsoft Excel; MatLab etc

IMARIS, Excel and Matlab have been replaced by generic terms (image analysis software, spreadsheet software, data analysis software). These software were referenced in the Material List.

9. Please ensure that the references appear as the following: [Lastname, F.I., LastName, F.I., LastName, F.I. Article Title. Source (ITALICS). Volume (BOLD) (Issue), FirstPage–LastPage (YEAR).] For 6 and more than 6 authors, list only the first author then et al. Please include volume and issue numbers for all references, and do not abbreviate the journal names. Ref 3 does not have any page numbers.

Ref 3 was corrected.

Points 5, 6, 7, 8 and 10 were verified.

Reviewers' comments:

Reviewer #1:

Manuscript Summary:

Here, Boutillon and colleagues describe a method by which a two-photon microscope is used to ablate tissues deep within zebrafish embryos. Laser ablation studies are extremely useful for examining physical forces within embryonic tissues. However, many laser ablation methods rely on UV radiation, which is effective in tissues near the surface of a sample but not deep within it. The present manuscript overcomes these limitations using two-photon illumination, which penetrates deeper into tissues and allows ablation to be focused to regions well defined in all three dimensions. This method also spares overlying superficial tissues, preventing confounding effects from off-target tissue damage. The authors demonstrate this approach by transecting the polster of gastrulating zebrafish embryos, which they accomplish without damaging the underlying yolk or the overlying ectoderm layer. They also document evidence of unsuccessful ablations, which will be especially helpful for readers attempting to recreate these methods. Overall, this is a clear and detailed description of a very useful technique that I anticipate will be of value to the zebrafish community. I have only minor comments to improve clarity, which are outlined below.

Minor Concerns:

1. Some language in the abstract and the first part of the introduction is confusing. Some examples are below:

- Line 22: "Morphogenesis implies many cell movements to organize…"

- Lines 40-43: The start of the intro is two run-on sentences whose meanings are difficult to understand.

- Line 86: "A better understanding… implies removing some cells,"

We have modified the text to, hopefully, clarify these sentences.

A couple other small points within the abstract:

- Line 30: Indicate that these are zebrafish transgenic lines.

- Line 31: "The forming axis" - recommend specifically indicating the axial mesoderm.

Abstract was modified accordingly.

2. Section 4.6: The authors say to orient the embryo so the targeted region is at the top, and in the representative results say the embryo was mounted so the "plane of the polster is perpendicular to the optical axis". Because proper positioning is so critical to this method, perhaps the authors could include a diagram in Figure 1 showing the angle at which the embryo should be mounted with respect to the objective lens.

We thank the reviewer for this suggestion and have included a scheme of embryo mounting as Figure 1B.

3. Throughout section 5, the authors refer to focal planes using terms like: "top, above, below, highest, and lowest". Because these are relative positions depending on the configuration of

the microscope and sample, more subjective terms like "animal/vegetal" and "deep/superficial" would be preferable.
We tried to clarify the text, referring to deep and superficial as suggested.

4. Line 256 states that if cavitation occurs, "treatment should be turned down". How is this achieved? By adjusting laser power?
We agree this is an important precision. While both approaches (reducing laser power of reducing the number of treatments) are feasible, we prefer adjusting the number of treatments. This is now specified in the sentences dealing with cavitation (as suggested), as well as in the sentences dealing with photobleaching.

5. Line 284 refers to "GFP cytoplasmic staining and mCherry nuclear staining". However, these are fluorescent proteins expressed either from a transgene or injected RNA, and therefore are not "staining" anything. Recommend replacing "staining" with "signal".
We agree and have replaced “staining” with “signal”.

6. Consider recoloring Figures 1 & 3 with color blind-friendly combinations such as green/magenta instead of green/red.
Figures 1 and 3 as well as Movie S1 have been modified to green/magenta instead of green/red.

Reviewer #2:
Manuscript Summary:
The article "Deep and spatially controlled volume ablations using a two-photon microscope in the zebrafish gastrula." by Boutillon et al. is a very well written protocol on cell ablation by a 2-photon system in zebrafish. I have only some minor comments.

100 - I believe that embryo medium (EM) refers to ERM (embryonic rearing medium, E15) defined in the "The Zebrafish Handbook"? Please clarify.
As indicated in the Material List, EM refers to Embryo Medium, as described in ‘The zebrafish book’ by Monte Westerfield (http://zfin.org/zf_info/zfbook/zfbk.html). This was referenced in the Material List, but may not have been visible, as the Material List is split on two pages in the automatically generated pdf file.

109 - "collect fertilized eggs" - how can one distinguish between fertilized and unfertilized eggs at this stage?
We agree that it is not possible to distinguish fertilized and unfertilized eggs at this stage. We have thus removed ‘fertilized’ from the sentence.

118 - "RNA solution" should be changed to "mRNA solution."
This was corrected.

388 - Laser ablations are one of the few available techniques to remove or destroy structures

physically. I can't entirely agree with this statement as the cell debris could release cytokines and signalling molecules influencing the development of the surrounding tissue.

We agree that laser ablation are not equivalent to physical removal, as they leave some cell debris, that may physically or chemically impact neighbouring cells. The discussion paragraph was thus modified to distinguish physical removal from ablation and discuss the potential differences.

General comments:
A similar experiment has been performed recently by Bosze et al. 2020 and should be cited in the article.

The reference was added in the discussion.

Finally, cell ablation is obviously an established experimental concept in developmental biology. However, I would like to see a more critical discussion about the pros and cons of this technique compared to other methods such as the physical removal of cells. One of the most critical examples of cell ablation versus separation in the history of developmental biology should be discussed, namely the blastomere destruction experiments in frogs from Wilhelm Roux (theory of development). Hans Driesch challenged this hypothesis in sea urchins by physical separation of blastomeres with a completely different outcome.
The discussion paragraph was modified to point that ablations destroy cells and may thus release cytoplasmic content, which can influence neighboring cells (as illustrated by the Roux/Driesch controversy, or by differences in wound healing assays between scratch induced wounds and wounds created by removal of an insert).

Reviewer #3:
Manuscript Summary:
In this article Boutillon et al. give a detailed description of the use of a two-photon microscope setup to perform laser ablations in live zebrafish embryos. The article is well explained with a large amount of detail included which would allow other researchers to repeat the experiment as well as suggesting common potential errors regarding selecting treatment conditions to successfully perform an ablation. They also provide a justification of why this method would be preferred over other methods to achieve the desired results. Below are some minor concerns that should be addressed before publication.

Minor Concerns:
1. It would be interesting to know the rationale of using 820nm wavelength for laser ablation. Did the authors try different wavelengths with different success rates? Have other studies used 820nm with a 2-photon laser on a comparable biological tissue?
The 820 nm wave-length was chosen because it is the wave-length for which we reach highest peak energy out of the lens (due both to characteristics of our laser and of our optics which are optimized for this wavelength). Peak energy appears as the main parameter affecting plasma generation, and hence ablation efficiency. The precise wave-length does not seem to be a key parameter, as NIR ablations have been successfully performed at wave-lengths

ranging from 800 nm to 1030 nm. This important point and the associated references have been added to the manuscript.

2. It seems that multiple treatments were used at different focal planes (Table1), so the ablation might take a considerable amount of time. It would be good to know how long the total treatment takes to cut through the entire tissue. As the authors stated, the cells are moving (~3 um/min), so potentially different cells are ablated if the treatment time exceeds the time for cells to move out of the target frame.
This is an important point, which we have now specified in the discussion. Severing of the polster is achieved in 2 to 3 minutes (which could be lowered a bit by optimizing and automating the software). We added a sentence to point that cells may enter or exit the targeted area during the procedure. This could be an issue if absolute cell resolution was required. It is not for polster severing.

3. The authors show that laser ablation affects the correlation and migration of cells within the tissue. However, they also show that embryos show no obvious morphological phenotype 24 hours later. It seems as severing the tissue would only have a short time impact on tissue development? How long does loss of migration last after ablation?

The effect of laser ablation is permanent in the sense that some cells have been destroyed, which is irreversible. The fact that embryos develop fine after severing of the polster is a very intriguing observation, that raises important biological questions on how polster cells migrate. To answer the reviewer's question, our observation is that after severing, cells in the anterior, isolated part of the polster, are less correlated, and actually migrate less towards the animal pole. This is, however, not the case of cells in the posterior half, which keep migrating towards the animal pole, leading to a healing of the gap created by laser ablation in 20 to 30 minutes. After healing, all cells resume a normal migration towards the animal pole. Why anterior cells and not posterior ones are affected, and why anterior cells resume migration after healing are questions we have addressed in

Guidance by followers ensures long-range coordination of cell migration through α-Catenin mechanoperception
Arthur Boutillon, Diego Jahn, Sebastián González-Tirado, Jörn Starruß, Lutz Brusch, Nicolas B. David
bioRxiv 2021.04.26.441407; doi: https://doi.org/10.1101/2021.04.26.441407

We however feel that this is a complex biological question, which is out of the scope of this technical article, which is why we decided to simply demonstrate how cell migration properties can be measured, but not discuss the biological implications of these observations.

4. In Fig. 3, the authors do not mention the use of a non-ablated control embryo. Comparing to a non-treated embryo would be necessary to estimate differences in autocorrelation at similar developmental times in non-ablated embryos.
We had used the pre-ablation measurements as a control, but agree with the referee that cell behavior may vary in time (it actually does vary a bit). We have thus now included on Figure 3B the direction auto-correlation of cells forming the anterior half of the polster in a non-ablated embryo, at stages equivalent to those analyzed in ablated embryos.

5. 6.4 (line 193) refers to 3.2 (line 124) instead of 3.3 (line 127).
The power changes format from 300mW to 0.3W which could cause confusion.
This was corrected, thanks for pointing.

6. Line 341 refers to Fig. 2 when I believe it should refer to Fig. 3.
This was corrected, thanks for pointing.

7. For a readership not familiar with the system used here it would be informative to include some more references of studies that have previously imaged this system such as Johansson M. et al. 2019 Dev Cell, Smutny M. et al. 2017 Nat Cell Biol, etc. Although it appears that laser ablation was not used, these studies have performed similar analysis of cell speed and orientation.
Along the same lines, it would help readers who are not so accustomed with laser ablation setups to include some more references on NIR/UV laser ablation.

Suggested references and a few additional ones describing polster migration were added to the introduction. References on NIR and UV laser ablations were also added in the introduction. Hopefully this will help the reader.